SEMI-ANNUAL STATUS REPORT

Submitted to: NASA Marshall Space Flight Center

Grant Title: Theory and Computation of Optimal Low- and Medium-Thrust Transfers

Grant Number: NAG8-921

Principal Investigator
/Project Director: Dr. C.-H. Chuang
School of Aerospace Engineering
Georgia Institute of Technology
Atlanta, GA 30332-0150
Phone: (404) 894-3075
Fax: (404) 894-2760
E-mail: ch.chuang@aerospace.gatech.edu

Research Assistant: Troy Goodson
School of Aerospace Engineering
Georgia Institute of Technology

Period Covered: July 7, 1993 to January 6, 1994

Date of Submission: January 4, 1994

TABLE OF CONTENTS

Numerical Computation of Fuel-Optimal, Low- and Medium- Thrust Orbit Transfers in Large Numbers of Burns

ABSTRACT

This report presents two numerical methods considered for the computation of fuel-optimal, low-thrust orbit transfers in large numbers of burns. The origins of these methods are observations made with the extremal solutions of transfers in small numbers of burns; there seems to exist a trend such that the longer the time allowed to perform an optimal transfer the less fuel that is used. These longer transfers are obviously of interest since they require a motor of low thrust; however, we also find a trend that the longer the time allowed to perform the optimal transfer the more burns are required to satisfy optimality. Unfortunately, this usually increases the difficulty of computation.

Both of the methods described use small-numbered burn solutions to determine solutions in large numbers of burns. One method is a homotopy method that corrects for problems that arise when a solution requires a new burn or coast arc for optimality. The other method is to simply patch together long transfers from smaller ones. An orbit correction problem is solved to develop this method. This method may also lead to a good guidance law for transfer orbits with long transfer times.

I. INTRODUCTION

Electric propulsion, with its high specific impulse, promises very low fuel consumption but it produces less thrust than its counterparts. If one wants to use electric propulsion, one needs to be prepared to tolerate the long transfer times that will be incurred. The greater time spent thrusting must be spent wisely if fuel savings are to

realized. Furthermore, the effects of Earth's oblateness and atmospheric drag become more significant on the orbits of long transfer times.

To spend the thrusting time wisely, we form an optimal control problem to maximize the mass at the end of the transfer. This, therefore, is our cost function

$$J = m(t_f) \tag{1}$$

subject to the boundary conditions

$$\psi\left(\mathbf{r}(0), \mathbf{v}(0), \mathbf{r}\left(t_f\right), \mathbf{v}\left(t_f\right)\right) = 0 \tag{2}$$

and the state dynamics

$$\dot{\mathbf{r}} = \mathbf{v} \tag{3}$$

$$\dot{\mathbf{v}} = \frac{T}{m}\mathbf{e}_T - \frac{\mu}{r^3}\mathbf{r} \tag{4}$$

$$\dot{m} = -\frac{T}{g_o I_{sp}} \tag{5}$$

where $\mathbf{e}_T$ is the thrust direction, a unit vector, and the thrust magnitude, T, is limited between zero and some maximum value T_{max}, μ is the gravitational constant, g_o is the gravitational acceleration at sea-level, and I_{sp} is the specific impulse of the motor. Sometimes $g_o I_{sp}$ is referred to as the exit velocity of the motor. If the boundary conditions referred to in Eqn. (2) are designed for the rendezvous problem, this results in the well-known bang-bang optimal control problem, discussed in detail by Lawden[1]. However, herein the boundary conditions are designed such that the initial and final points lie on the desired orbits without specifying the position, or true anomaly, on either orbit.

As a brief review, the optimal thrust direction for this problem is

$$\mathbf{e}_T = \frac{\lambda_\mathbf{v}}{|\lambda_\mathbf{v}|} \tag{6}$$

where $\lambda_\mathbf{v}$ is found from the following differential equations

$$\dot{\lambda}_r = \mu\left[\frac{\lambda_v}{r^3} - 3\frac{(\lambda_v{}^T \mathbf{r})\mathbf{r}}{r^5}\right] \tag{7}$$

$$\dot{\lambda}_v = -\lambda_r \tag{8}$$

$$\dot{\lambda}_m = \frac{T}{m^2}\lambda_v{}^T \mathbf{e}_T = \frac{T}{m^2}|\lambda_v| \tag{9}$$

The optimal thrust magnitude for this problem is a bang-bang solution. This is determined by applying the following switching law, Eqn. (10), to the switching function, Eqn. (11).

$$\begin{aligned} &H_S > 0, \quad T = T_{max} \\ &H_S < 0, \quad T = 0 \end{aligned} \tag{10}$$

$$H_S = \frac{|\lambda_v|}{m} - \frac{\lambda_m}{g_o I_{sp}} \tag{11}$$

We are interested in solutions of this problem with long transfer times and, therefore, large numbers of burns. There are many methods that have been successively used to compute n-burn transfers, where n is anywhere from 1 to about 6. However, fewer methods successively compute transfers for larger values of n. These methods for the former attempt to solve the optimal control problem either directly, indirectly, or with a hybrid of the two. In this report, we will assume that a mostly indirect method, such as BOUNDSCO or MBCM or that of Brusch[2], et. al, or of Redding[3] is being used.

One idea to obtain interesting solutions is to first compute some n-burn transfer, where n is generally less than the number of burns initially desired. Using this as a starting point, increase the allowed transfer time and compute the new transfer. Obviously, it is expected that the desired transfer is relatively similar to the starting transfer. This homotopy method seems to work well as long as the number of burns performed in the transfer do not need to increase so that optimality is satisfied. For example, in many cases BOUNDSCO is unable to find a three burn solution when the two burn solution to an almost identical problem is given as the initial guess. The Direction Correction Method has been developed to attempt to alleviate this difficulty. It's purpose is to find an n burn solution to an orbit transfer problem with allowed

transfer time $t_f + \delta t_f$ using an n-1 burn solution to the same problem but with allowed transfer time t_f.

Another idea is to patch together a set of n-burn transfers, where n is a small integer, usually unity, to produce an m-burn transfer, where m is the desired number of burns. This method requires that the sequence of transfer orbits be either guessed and iterated upon for optimality, or simply prespecified. From the theory of optimal control, this patched solution will be a suboptimal solution. However, possible analytical solutions for the one burn solution of two very close orbits may give a feedback guidance law. Since the drag model is only approximate for large numbers of burns it may be more important to have a good guidance law in terms of fuel-savings.

II. Direction Correction Method

The first idea, referred to herein as the Direction Correction Method, is based on the common homotopy strategy. A homotopy method, though slow in producing results, would be considered effective here as long as the number of burns does not change. It is expected, however, that one is going to be using this method to increase the transfer time so that the fuel consumed will be less. To understand the ensuing difficulty, we must study the history of a successful implementation of this homotopy method.

All parameters describing transfers in this section and below have been nondimensionalized such that the gravitational constant, μ, is unity. This nondimensionalization is accomplished through two parameters, $r^{\star}$ and $m^{\star}$ with units of length and mass, respectively. These are chosen appropriately to the problem and may be, for example, initial semimajor axis and initial mass, respectively. The following equations detail the calculation of nondimensional parameters, denoted by the '^' symbol, describing the transfer:

$$\hat{T} \equiv \frac{T/m^{\star}}{\mu/r^{\star 2}} \tag{12a}$$

$$(\hat{g}_o \hat{I}_{sp}) \equiv g_o I_{sp} \sqrt{r^{\star}/\mu} \tag{12b}$$

$$\hat{t}_f \equiv \frac{t_f}{\sqrt{r^{\star 3}/\mu}} \tag{12c}$$

The optimal transfer we will examine is a planar transfer under ideal gravity conditions. The transfer leaves an initial orbit with a semimajor axis of 2.239, eccentricity of 0.1160, and an argument of perigee of -85.94°. The orbit to be entered has a semimajor axis of 7.000, eccentricity of 0.7332, and an argument of perigee of 114.6°. The motor used to perform the transfer delivers a thrust of 0.01386 with an exit velocity of 0.3898. The allowed transfer time is 73.33. This transfer performed in two burns is shown in Figure 1 with its corresponding parameters in Table I. It was computed using the multiple-shooting method of BOUNDSCO[4]. The switching function for this transfer is shown in Figure 2a.

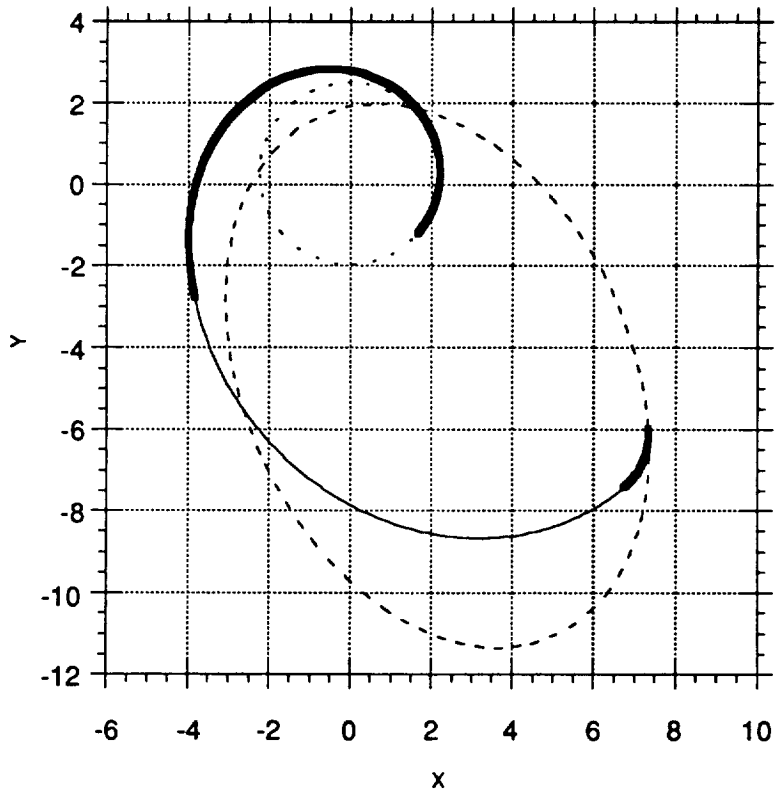

Figure 1. Transfer in Two Burns for Burn Addition Demonstration

$g_o I_{sp}$ =	0.3898	a_i=	2.239	ω_i=	-85.94°	a_f=	7.000	ω_f=	114.6°
T=	0.01386	e_i=	0.1160	t_f=	73.33	e_f=	0.7332	m_f=	0.5545

Table I. Parameters of the transfer shown in Figure 1

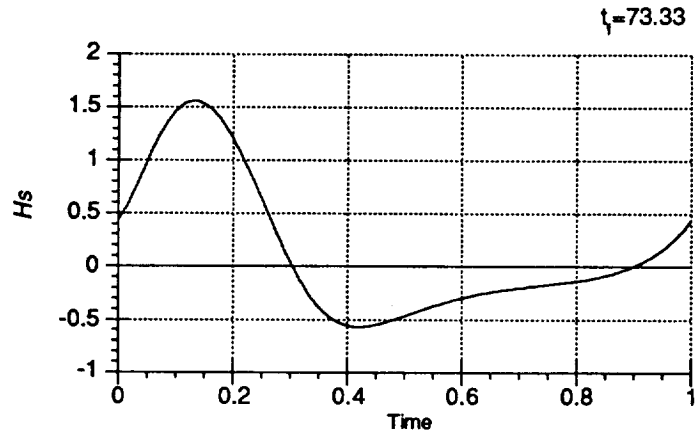

Figure 2a Switching Function for a Two Burn Transfer

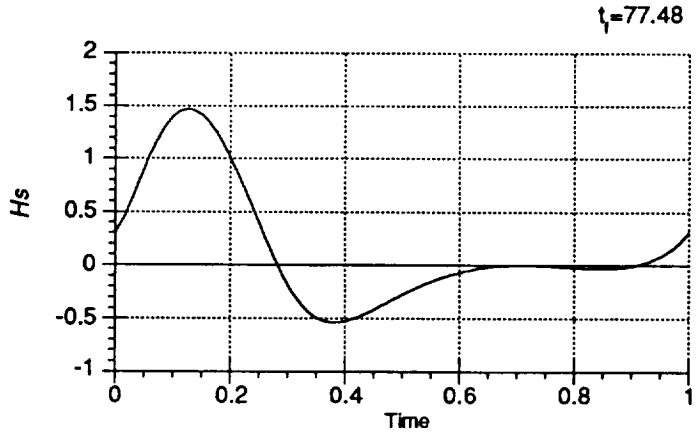

Figure 2b Switching Function for a Two or Three Burn Transfer

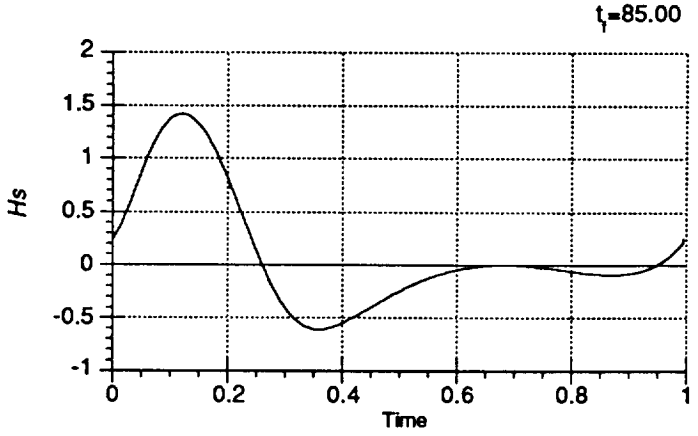

Figure 2c Switching Function for a Three Burn Transfer

The initial mass of the spacecraft was 1.6, the final mass is 0.5545. Now, suppose that a greater fuel savings is desired. As the allowed transfer time is increased from 73.33 to 77.48 and then to 85.00, the shown sequence of switching functions ($H_S(t)$ in Figs. 2a-c) will result. These show a clear indication of a new burn/coast being anticipated in the optimal solution. The orbit transfer corresponding to the switching function in Fig. 2c is plotted in Figure 3. The parameters of this transfer are identical to that of Fig. 1 except that the transfer time is longer, t_f=85, see Table II for the listing. Also, note that the final mass of this longer transfer is indeed larger than the shorter transfer, indicating a greater fuel savings.

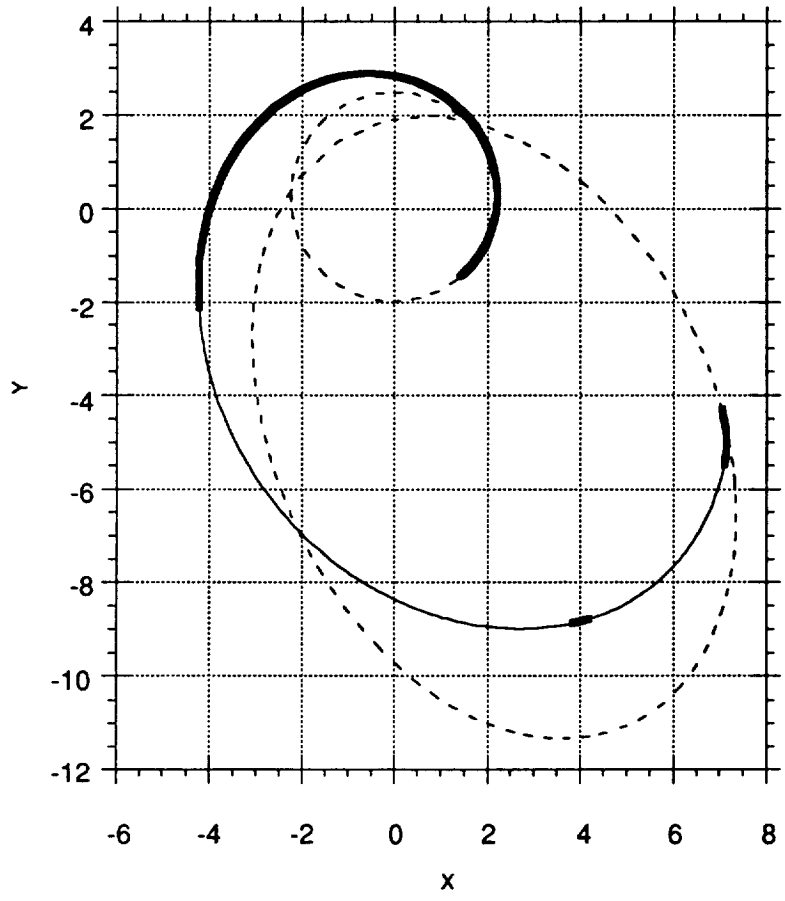

Figure 3 Transfer in Three Burns for Burn Addition Demonstration

$g_o I_{sp}$ =	0.3898	a_i=	2.239	ω_i=	-85.94°	a_f=	7.000	ω_f=	114.6°
T=	0.01386	e_i=	0.1160	t_f=	85.00	e_f=	0.7332	m_f=	0.6056

Table II. Parameters of the transfer shown in Figure 3

It has been seen in many cases that local minima and maxima of the switching function will move down or up on the graph as we examine successive solutions. As in Fig. 2b, once this critical point becomes a root of the switching function, we reach a point where the number of burn/coasts is somewhat indeterminate. Is this, in Fig. 2b, a two- or three- burn extremal? There are only two burns of finite length but there is a third that is infinitely small. This indeterminacy shows itself as a discontinuity in the slope of a plot of the initial guess versus the homotopy variable, transfer time, Figure 4.

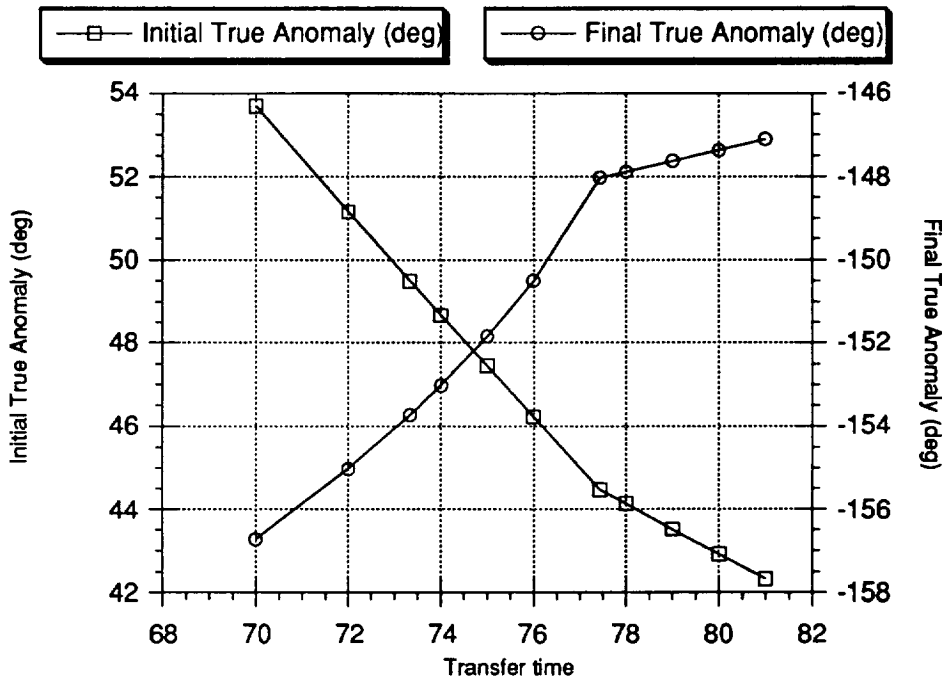

Figure 4 **Plot of Initial and Final True Anomaly Values of Successive Solutions which Differ only in Transfer Time, t_f.**

Figure 4 shows the initial and final true anomalies as a function of the allowed transfer time. The feature of interest here is the slope discontinuity (note that there is no point discontinuity) in both curves. The effect is not as prominent for the initial true anomaly as it is for the final, but it is still noticeable. As a result of this discontinuity there is difficulty in the homotopy method: the next solution may not converge because the method being used, based on the linear slope of previous points, is not calculating the correct initial state. To overcome this difficulty we must be able to compute the correct

slope, which should be the slope after t_f = 77.48, so that the homotopy method can continue.

The change in the initial state needs to be computed such that satisfaction of the boundary conditions is maintained and optimality is preserved. This problem shall be approached for the following general Two-Point-Boundary-Value-Problem (TPBVP):

$$\mathbf{C}(\mathbf{z}(0)) = 0 \quad m \text{ equations} \tag{13a}$$

$$\mathbf{D}\left(\mathbf{z}\left(t_f\right)\right) = 0 \quad m - n \text{ equations} \tag{13b}$$

$$\dot{\mathbf{z}}(t) = \mathbf{f}(\mathbf{z}(t)) \quad n \text{ equations} \tag{13c}$$

where $\mathbf{z}(t)$ is the state consisting of the original state plus the Lagrange multipliers, $\mathbf{f}(t)$ is the right-hand side of the original state dynamics plus the Euler-Lagrange equations, and $\mathbf{C}(\mathbf{z}(0))$ and $\mathbf{D}(\mathbf{z}(t_f))$ are the boundary conditions for the initial and final orbits, respectively.

Now, since we are interested in maintaining the boundary conditions, we set their variations equal to zero. First, the initial conditions from Eqn. (13a):

$$\delta\mathbf{C} = \left.\frac{\partial \mathbf{C}}{\partial \mathbf{z}}\right|_{\mathbf{z}(0)} \delta\mathbf{z}(0) = 0 \tag{14}$$

Next, a similar operation is performed on a vector describing the final conditions from Eqn. (13b). However, so that the initial state is referred to, it is necessary to invoke the transition matrix.

$$d\mathbf{D} = \left.\frac{\partial \mathbf{D}}{\partial \mathbf{z}}\right|_{\mathbf{z}(t_f)} d\mathbf{z}\left(t_f\right) = 0 \tag{15a}$$

$$= \left.\frac{\partial \mathbf{D}}{\partial \mathbf{z}}\right|_{\mathbf{z}(t_f)} \left(\delta\mathbf{z}\left(t_f\right) + \dot{\mathbf{z}}\left(t_f\right) dt_f\right) \tag{15b}$$

$$= \left.\frac{\partial \mathbf{D}}{\partial \mathbf{z}}\right|_{\mathbf{z}(t_f)} \Phi\left(0, t_f\right)\delta\mathbf{z}(0) + \left.\frac{\partial \mathbf{D}}{\partial \mathbf{z}}\right|_{\mathbf{z}(t_f)} \dot{\mathbf{z}}\left(t_f\right) dt_f = 0 \tag{15c}$$

Here, $d(\cdot)$ denotes a variation with variable time and $\Phi(0,t_f)$ is defined as the transition matrix, initialized at t=0, and evaluated at t=t_f, where

$$\dot{\Phi}(t_o,t) = \left.\frac{\partial \mathbf{f}(\mathbf{z}(t))}{\partial \mathbf{z}(t_o)}\right|_{\mathbf{z}(t)} \Phi(t_o,t) \tag{16a}$$

$$\Phi(t_o,t_o) = \mathbf{I} \tag{16b}$$

Now at each switching time, t_i (i=0,1...q), the switching function must be satisfied. So, we set the variation of the switching function, $H_S(\mathbf{z})$, equal to zero at each switching time, giving q scalar equations:

$$dH_s = \left.\frac{\partial H_s}{\partial \mathbf{z}}\right|_{\mathbf{z}(t_i)} d\mathbf{z}(t_i) = 0 \tag{17a}$$

$$= \left.\frac{\partial H_s}{\partial \mathbf{z}}\right|_{\mathbf{z}(t_i)} \left(\Phi(0,t_i)\delta\mathbf{z}(0) + \dot{\mathbf{z}}(t_i)dt_i\right) = 0 \tag{17b}$$

$$= \left.\frac{\partial H_s}{\partial \mathbf{z}}\right|_{\mathbf{z}(t_i)} \Phi(0,t_i)\delta\mathbf{z}(0) + \left.\frac{\partial H_s}{\partial \mathbf{z}}\right|_{\mathbf{z}(t_i)} \dot{\mathbf{z}}(t_i)dt_i = 0 \tag{17c}$$

Consideration of the switching function also calls attention to a necessary correction in the transition matrix calculation. At each switching point, there is a discontinuity in $\mathbf{f}(\mathbf{z}(t))$ due to the thrust being turned on or off. This discontinuity results in a 'jump' term for $\Phi(0,t_f)$. To calculate this term, we again must set the total change in H_S equal to zero.

$$H_s(\mathbf{z}(t_i)) = 0 \tag{18a}$$

$$dH_s = \left.\frac{\partial H_s}{\partial \mathbf{z}}\right|_{\mathbf{z}(t_i)} d\mathbf{z}(t_i) = 0 \tag{18b}$$

Now, recognize that the total variation in the state at the switching time t_i must be the same looking from either direction. This situation is illustrated in Figure 5.

$$d\mathbf{z}(t_i) = \delta\mathbf{z}(t_i^-) + \dot{\mathbf{z}}(t_i^-)dt_i \tag{19a}$$

$$= \delta\mathbf{z}(t_i^+) + \dot{\mathbf{z}}(t_i^+)dt_i \tag{19b}$$

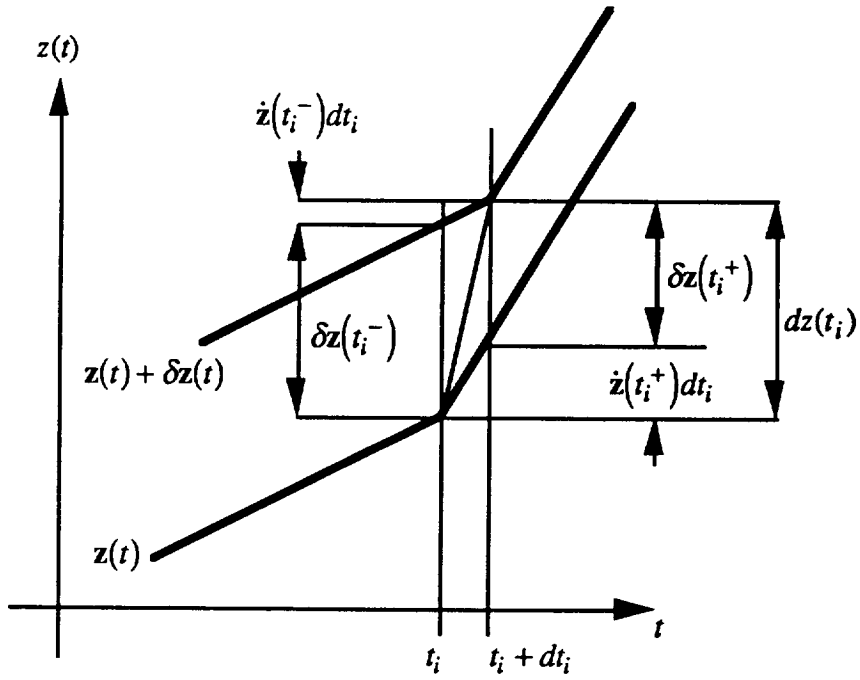

Figure 5. Illustration of Equations 19a and 19b

Substitute Eqn. (19b) into Eqn. (18b)

$$dH_s = \left.\frac{\partial H_s}{\partial \mathbf{z}}\right|_{\mathbf{z}(t_i)} \left(\delta \mathbf{z}(t_i^-) + \dot{\mathbf{z}}(t_i^-)dt_i\right) = 0 \tag{20}$$

Equation (13) can be solved immediately for dt_i which is then substituted into Eqns. (19a-b). This can manipulated to produce

$$\delta \mathbf{z}(t_i^+) = \delta \mathbf{z}(t_i^-) + \left(\dot{\mathbf{z}}(t_i^+) - \dot{\mathbf{z}}(t_i^-)\right) \frac{\left.\frac{\partial H_s}{\partial \mathbf{z}}\right|_{\mathbf{z}(t_i)} \delta \mathbf{z}(t_i^-)}{\left.\frac{\partial H_s}{\partial \mathbf{z}}\right|_{\mathbf{z}(t_i)} \dot{\mathbf{z}}(t_i^-)} \tag{21}$$

Equation (21) can be rewritten by inspection in terms of the transition matrix:

$$\Phi\left(t_i^+, t_i^-\right) = \left(\mathbf{I} + \frac{\left(\dot{\mathbf{z}}\left(t_i^+\right) - \dot{\mathbf{z}}\left(t_i^-\right)\right) \left.\frac{\partial H_s}{\partial \mathbf{z}}\right|_{\mathbf{z}(t_i)}}{\left.\frac{\partial H_s}{\partial \mathbf{z}}\right|_{\mathbf{z}(t_i)} \dot{\mathbf{z}}\left(t_i^-\right)} \right) \tag{22}$$

This is the jump matrix across the switching point t_i.

We must recognize that these variations are considered in a range of transfer times across which the number of switching points changes. Specifically, this is an addition of a burn or coast arc. The situation is illustrated in Figure 6. The assumed change in the switching function is shown at the top of the figure. The nominal solution's switching function has a touch point at t_c=t_a=t_b. The solution with a slight different transfer time has two new switching points, t_a + dt_a and t_b + dt_b. The assumed change in one element of the state vector is shown at the bottom of Figure 6. The derivative, $\dot{\mathbf{z}}(t)$, is assumed equal before and after the new addition and to the nominal value, $\dot{\mathbf{z}}(t_c)$. The slope during the new burn is denoted c. To relate the two solutions across the arc, we write the following equation.

$$\delta\mathbf{z}(t_b + dt_b) = \delta\mathbf{z}(t_a + dt_a) + \left(c - \dot{\mathbf{z}}(t_b)\right)\left(dt_b - dt_a\right) \tag{23}$$

This relation has been verified using data from the example presented here.

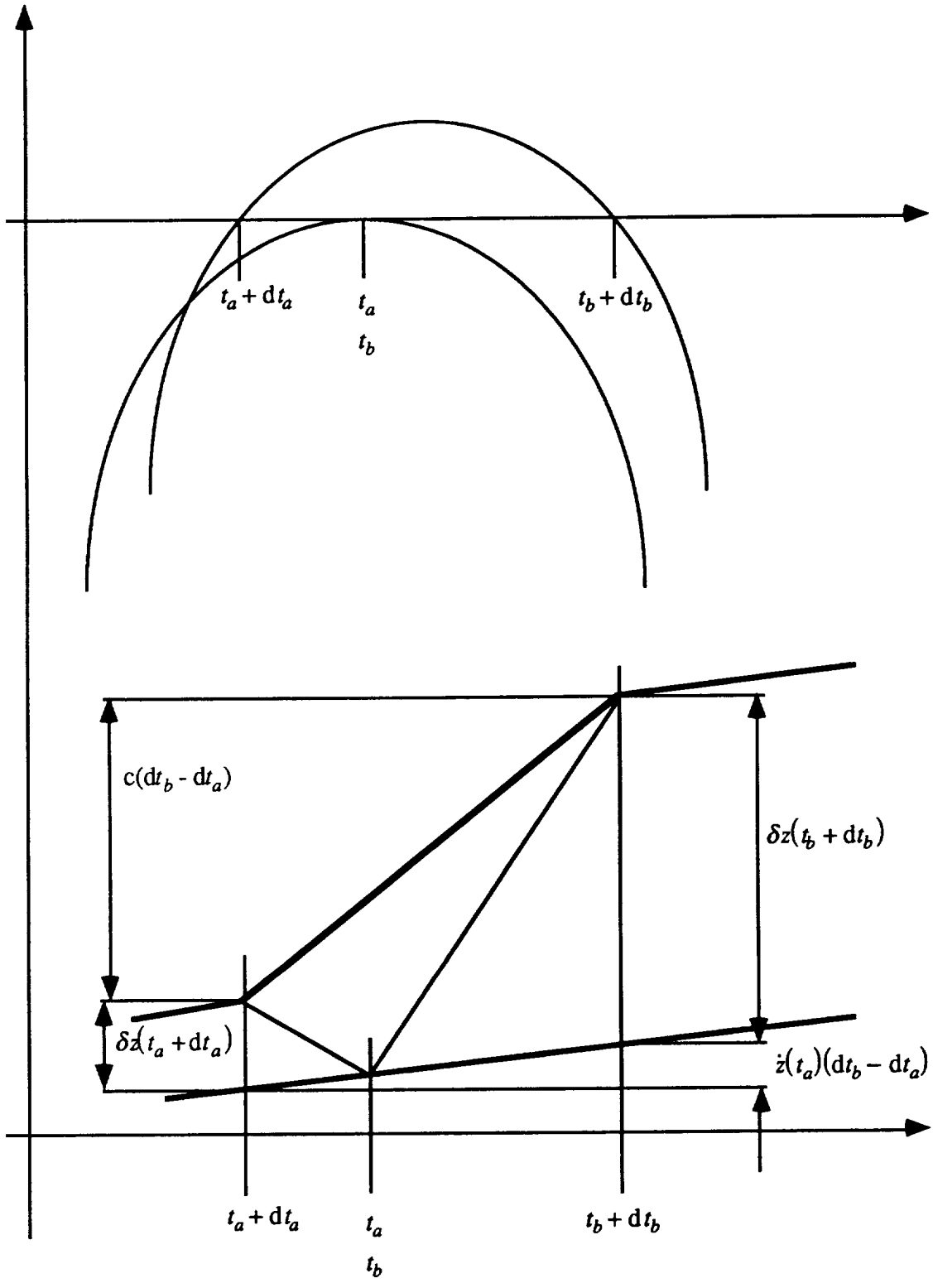

Figure 6: **Model Describing Changes Incurred Between *n* and *n+1* Burn Solutions**

Now, a model is required to locate the new switching points. We have looked into different models for this. The first model is a simple variational model, but unlike Eq (17a), second-order terms are considered. The equation of this model is

$$\Delta H_s \approx \frac{1}{2} d^2 H_s = \frac{1}{2} d\mathbf{z}(t_a)^{\mathrm{T}} \left.\frac{\partial^2 H_s}{\partial \mathbf{z} \partial \mathbf{z}}\right|_{\mathbf{z}(t_a)} d\mathbf{z}(t_a) = 0 \tag{24a}$$

$$= \frac{1}{2} \left(\delta \mathbf{z}(t_a) + \dot{\mathbf{z}}(t_a) dt_a\right)^{\mathrm{T}} \left.\frac{\partial^2 H_s}{\partial \mathbf{z} \partial \mathbf{z}}\right|_{\mathbf{z}(t_a)} \left(\delta \mathbf{z}(t_a) + \dot{\mathbf{z}}(t_a) dt_a\right) \tag{24b}$$

$$= \frac{1}{2} \left[\delta \mathbf{z}(t_a)^{\mathrm{T}} \left.\frac{\partial^2 H_s}{\partial \mathbf{z} \partial \mathbf{z}}\right|_{\mathbf{z}(t_a)} \delta \mathbf{z}(t_a) + 2 \delta \mathbf{z}(t_a)^{\mathrm{T}} \left.\frac{\partial^2 H_s}{\partial \mathbf{z} \partial \mathbf{z}}\right|_{\mathbf{z}(t_a)} \dot{\mathbf{z}}(t_a) dt_a \right.$$

$$\left. + \dot{\mathbf{z}}(t_a)^{\mathrm{T}} \left.\frac{\partial^2 H_s}{\partial \mathbf{z} \partial \mathbf{z}}\right|_{\mathbf{z}(t_a)} \dot{\mathbf{z}}(t_a) (dt_a)^2 \right] \tag{24c}$$

where the lesser of the two solutions is dt_a leaving the other to be dt_b. Unfortunately this model does not result in a sufficiently accurate answer for dt_a and dt_b.

We have also attempted to model the situation through the information on the placement of $t_c + dt_c$. Since this point can be defined as the point of zero slope, we can find with an analog of Eq. (17). The solution is, therefore,

$$dt_c = -\frac{\left.\frac{\partial \dot{H}_s}{\partial \mathbf{z}}\right|_{\mathbf{z}(t_c)} \delta \mathbf{z}(t_c)}{\left.\frac{\partial \dot{H}_s}{\partial \mathbf{z}}\right|_{\mathbf{z}(t_c)} \dot{\mathbf{z}}(t_c)} \tag{25}$$

To complete the model we need to have a point on the graph of ΔH_S and we need the curvature of H_S. The former can be had by rewriting Eq (17) for t_c and evaluating it at dt_c. We assume that the latter is well represented through a curve fit to the original switching function in the neighborhood of $H_S(t_c)$, denoted by k. in the following equation for ΔH_S.

$$\Delta H_s \approx k(t - t_c)^2 + \left(\left.\frac{\partial H_s}{\partial \mathbf{z}}\right|_{\mathbf{z}(t_c)} d\mathbf{z}(t_c) \right) \tag{26}$$

The solutions we are interested in are

$$dt_a = dt_c - \sqrt{\frac{\left(\left.\frac{\partial H_s}{\partial \mathbf{z}}\right|_{\mathbf{z}(t_c)} d\mathbf{z}(t_c)\right)}{k}} \tag{27a}$$

$$dt_b = dt_c + \sqrt{\frac{\left(\left.\frac{\partial H_s}{\partial \mathbf{z}}\right|_{\mathbf{z}(t_c)} d\mathbf{z}(t_c)\right)}{k}} \tag{27b}$$

We have found that the solutions with this model are better than that with the previous model, but still not very accurate with errors greater than 10%. However, this accuracy may still prove to be well enough for BOUNDSCO to produce solutions. The intention here is merely to provide the TPBVP solver an initial guess closer to the n+1 burn solution.

Taking all of this together, a system of linear and non-linear equations can be written, starting with Eqs (14) and (15)

$$\left.\frac{\partial C}{\partial \mathbf{z}}\right|_{\mathbf{z}(0)} \Phi(0, t_a + dt_a)\delta\mathbf{z}(t_a + dt_a) = 0 \tag{28a}$$

$$\left.\frac{\partial D}{\partial \mathbf{z}}\right|_{\mathbf{z}(t_f)} \Phi(t_b + dt_b, t_f)\mathbf{f}(\delta\mathbf{z}(t_a + dt_a)) = -\left.\frac{\partial D}{\partial \mathbf{z}}\right|_{\mathbf{z}(t_f)} \dot{\mathbf{z}}(t_f)dt_f \tag{28b}$$

where $\mathbf{f}(\delta\mathbf{z})$ refers to the right-hand side of Eq. (23) as a function of $\delta\mathbf{z}(t_a + dt_a)$. The solution to this system is $\delta\mathbf{z}(t_a + dt_a)$, The transition matrix can be used to give the change in the initial state required to produce the desired solution. Then the variation of each switching point can be found one at time using Eqn. (17c).

The solution information can easily be put into a form useful for a variety of numerical methods. For example, the change $\delta\mathbf{z}(0)$ can be propagated through the transition matrix to calculate the changes at each node point for a multiple point shooting method. This method is still under development but shows promise as relatively simple way of getting to the n+1 burn solution in the right direction.

Once we have the ability to find optimal solutions with successively increasing transfer times, there is another characteristic of the extremals that may be encountered. Experience has shown that the length of the new burn will increase monotonically as the

transfer time is increased and usually the situation detailed above will be repeated so that the number of burns will increase again. However, there are cases where the cycle ends and the transversality condition, giving the optimal transfer time, is satisfied and there may be no nearby solution that has better performance. The following solution is an example. It is a descent trajectory from an orbit with a semimajor axis of 3.847, eccentricity of 0.02378, and an argument of perigee of 0°. The transfer terminates at an orbit with a semimajor axis of 1.500, eccentricity of 0.3333, and an argument of perigee of 0°. The motor used to perform the transfer delivers a thrust of 0.03 with an exit velocity of 1.313. The allowed transfer time is 19.05. This transfer performed in two burns is shown in Figure 7a. It also was computed using the multiple-shooting method of BOUNDSCO. The switching function for this solution is shown in Figure 7b.

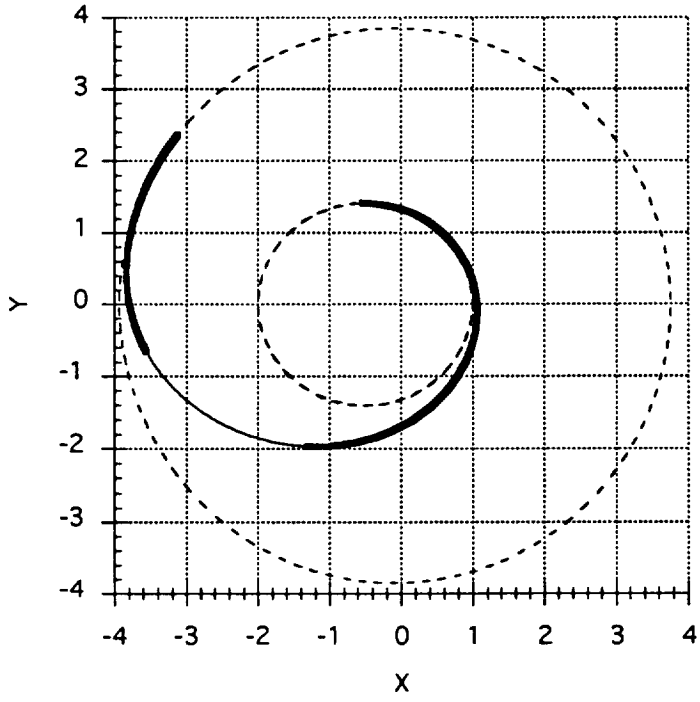

Figure 7a: Two Burn Extremal with Transversality Converged

$g_o I_{sp}$ =	1.313	a_i=	3.847	ω_i=	0.000°	a_f=	1.500	ω_f=	0.000°
T=	0.03	e_i=	0.02378	t_f=	19.05	e_f=	0.3333	m_f=	1.214

Table III. Parameters of the Transfer Shown in Figure 7

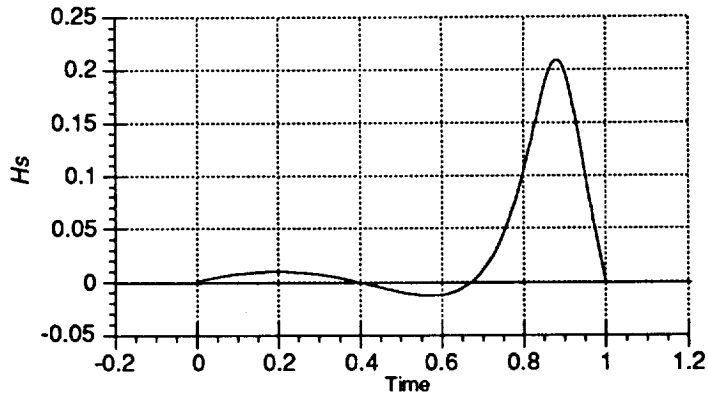

Figure 7b: Switching Function for Two Burn Extremal in Figure 7a

This solution was presented previously[5], however, with one difference, oblateness and atmospheric drag were included in the dynamics. It was found that with these terms removed, the transversality condition could be converged. It was also observed that the initial and final points of the switching function were driven to zero. There is certainly no conflict here in terms of optimality: the initial and final points are now switching points.

III. PATCHED TRANSFER METHOD

The second idea was inspired in part by the work of others. Zondervan, et. al made some simple guidance observations[6], specifically that in some regions the primer vector is relatively constant in a velocity-fixed reference frame. This implies that a simple control law is available in some cases. Marec presents a solution to the orbit correction problem[7]. This motivated a notion that solutions to linearized and/or approximated problems were available. In this spirit a solution was obtained for the optimal transfer between two close orbits. The transfer leaves a circular initial orbit with a radius of 1.038. The orbit to be entered has a semimajor axis of 1.069, eccentricity of 0.02633, and an argument of perigee of -50°. The motor used to perform the transfer delivers a thrust of 0.01438 with an exit velocity of 0.3861. The allowed transfer time is 1.553. This transfer is performed in one burn and is shown in Figure 8a. It was computed using the multiple-shooting method of BOUNDSCO. The switching function for this transfer is shown in Figure 8b.

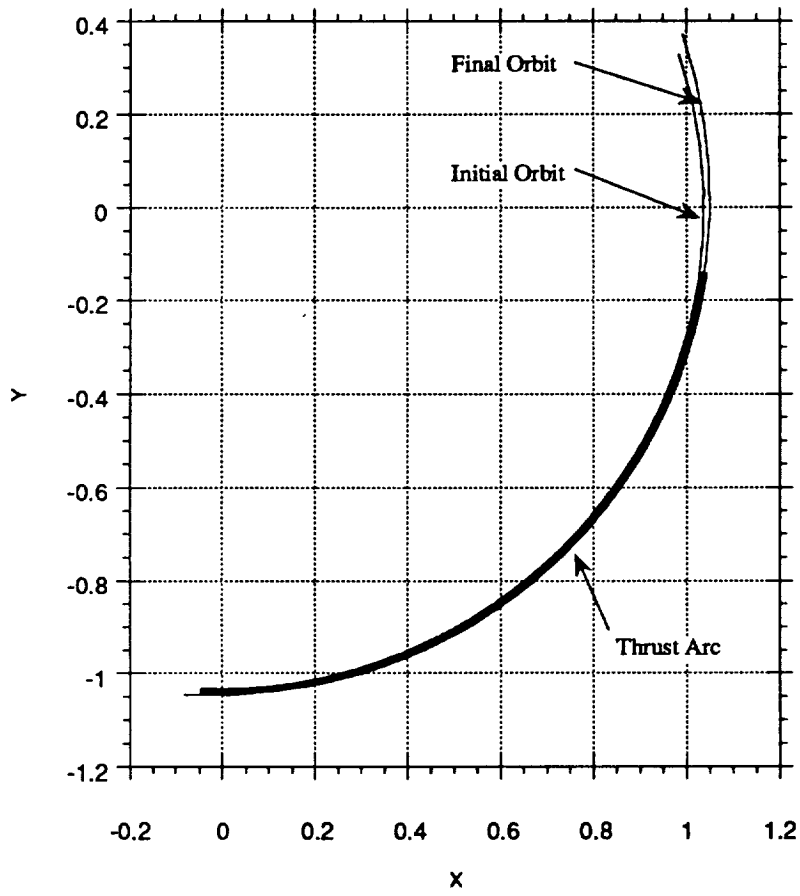

Figure 8a: One Burn Transfer Between Close Orbits: An Example of a Solution with a Simple Optimal Control

$g_o I_{sp}$ =	0.3861	a_i=	1.038	ω_i=	n/a	a_f=	1.069	ω_f=	-50°
T=	0.03	e_i=	0.000	t_f=	1.553	e_f=	0.02633	m_f=	1.542

Table IV. Parameters of the Transfer Shown in Figure 8a

Most interesting about this transfer is the simplicity of the control. Over this short transfer between a circular orbit and a close target orbit, the optimal control of the thrust angle is linear in time. And, in addition, we find that the control direction is almost coincident with the velocity direction.

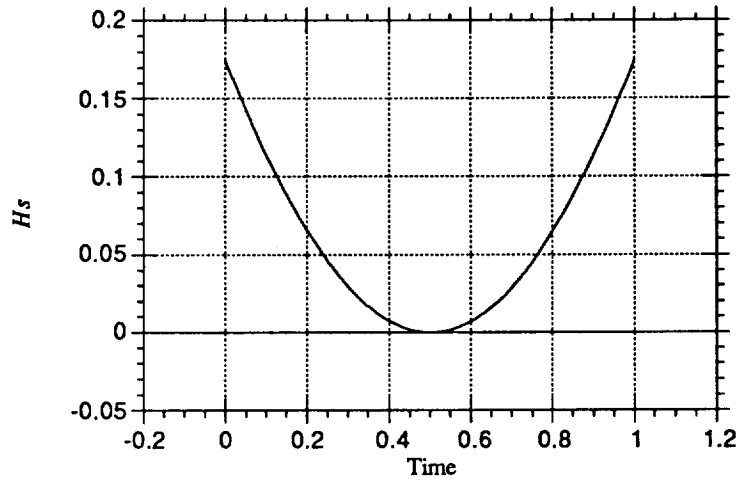

Figure 8b: Switching Function for One Burn Transfer Shown in Figure 8a

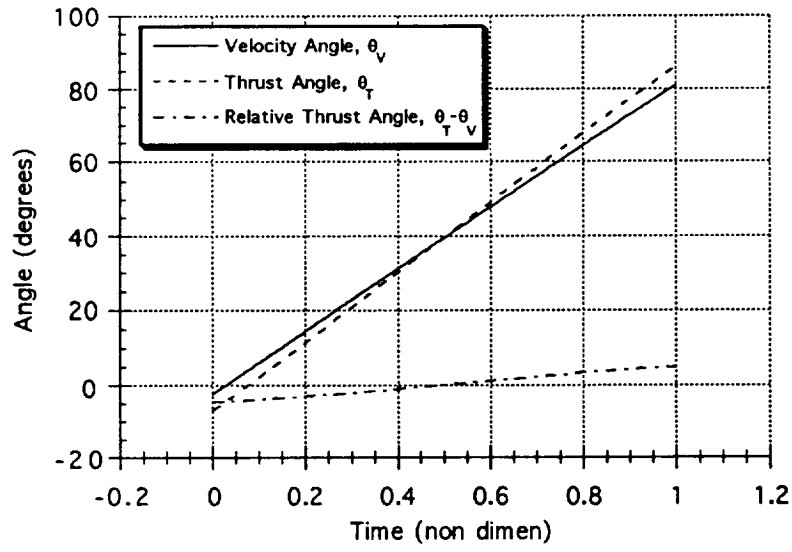

Figure 8: Plot of Thrust Direction, the Optimal Control, Alongside the Angle of the Velocity Vector.

To match this transfer analytically, a modified optimal control problem is considered. The dynamics for this problem are again the equations of orbital motion, however, this time the state is defined relative to the initial orbit. Assuming that the distance from the initial orbit is small compared to the radius of the initial orbit, we

ignore all terms to the order of $(\delta r/\rho)^2$. This assumption results in the following dynamics:

$$\delta\dot{\mathbf{r}} = \delta\mathbf{v} \tag{29a}$$

$$\delta\dot{\mathbf{v}} = \frac{T}{m}\mathbf{e}_T + 3\frac{\mu(\delta\mathbf{r}\bullet\rho)}{\rho^5}\rho - \frac{\mu}{\rho^3}\delta\mathbf{r} \tag{29b}$$

$$\dot{m} = -\frac{T}{g_o I_{sp}} \tag{29c}$$

Here, $\delta\mathbf{r}=[x\ y]^T$ and $\delta\mathbf{v}=[u\ v]^T$, $\mathbf{e}_T$ is the thrust direction, T is the thrust, m is the mass, μ is the gravitational constant, and ρ represents the initial orbit which satisfies identical dynamics but without the thrust term. Now, assuming that the initial orbit is circular, these can be rewritten as:

$$\dot{x} = u \tag{30a}$$

$$\dot{y} = v \tag{30b}$$

$$\dot{u} = \frac{T}{m}e_x + \frac{\mu}{\rho^3}\left[3(x\cos(\omega t) + y\sin(\omega t))\cos(\omega t) - x\right] \tag{30c}$$

$$\dot{v} = \frac{T}{m}e_y + \frac{\mu}{\rho^3}\left[3(x\cos(\omega t) + y\sin(\omega t))\cos(\omega t) - y\right] \tag{30d}$$

$$\dot{m} = -\frac{T}{g_o I_{sp}} \tag{30e}$$

Writing the Hamiltonian for this system and evaluating the Euler-Lagrange equations results in the following differential equations involving the costates:

$$\dot{\lambda}_u = -\lambda_x \tag{31a}$$

$$\dot{\lambda}_v = -\lambda_y \tag{31b}$$

$$\dot{\lambda}_x = -\lambda_u\frac{\mu}{\rho^3}\left(3\cos^2(\omega t) - 1\right) - \lambda_v\frac{\mu}{\rho^3}3\cos(\omega t)\sin(\omega t) \tag{31c}$$

$$\dot{\lambda}_y = -\lambda_u\frac{\mu}{\rho^3}\left(3\cos(\omega t)\sin(\omega t)\right) - \lambda_v\frac{\mu}{\rho^3}\left(3\sin^2(\omega t) - 1\right) \tag{31d}$$

$$\dot{\lambda}_m = -\frac{T}{m^2\sqrt{\lambda_u{}^2 + \lambda_v{}^2}} \tag{31e}$$

We also learn that the control, $\mathbf{e}_T$ is

$$\mathbf{e}_T = \frac{1}{\sqrt{\lambda_u{}^2 + \lambda_v{}^2}} \begin{bmatrix} \lambda_u \\ \lambda_v \end{bmatrix} \tag{32}$$

and the control T is bang-bang, governed by the switching function, H_T, as

$$H_T = \frac{\sqrt{\lambda_u{}^2 + \lambda_v{}^2}}{m} - \frac{\lambda_m}{g_o I_{sp}} \tag{33}$$

$$\begin{aligned} H_T > 0, \quad T = T_{max} \\ H_T < 0, \quad T = 0 \end{aligned} \tag{34}$$

Pleasantly, Eqns. (31) happen to be the equations for the costates on a coast arc coinciding with the initial orbit. In fact, this result is not limited to the assumption of a circular orbit. The coast arc costates have been solved by Lawden and other authors[8,9]. It also can be shown that Eqns. (31) are, in fact, identical to Eqns. (30), without the thrust terms, up to sign. Therefore, once we solve the system in Eqns. (31) we have the homogeneous solution to the system in Equations (30). Now to solve the differential Eqns (26), they must first be rewritten in a more useful form:

$$\begin{bmatrix} \dot{\lambda}_x \\ \dot{\lambda}_y \end{bmatrix} = -\begin{bmatrix} \ddot{\lambda}_u \\ \ddot{\lambda}_v \end{bmatrix} = -3l \begin{bmatrix} cos(\omega t) \\ sin(\omega t) \end{bmatrix} \begin{bmatrix} cos(\omega t) & sin(\omega t) \end{bmatrix} \begin{bmatrix} \lambda_u \\ \lambda_v \end{bmatrix} + l \begin{bmatrix} \lambda_u \\ \lambda_v \end{bmatrix} \tag{35}$$

where $l \equiv \mu/\rho^3 = \omega^2$. Now, define vectors $\mathbf{e}_\rho(t)$ and $\mathbf{e}_\omega(t)$, as the radial and circumferential directions associated with the initial orbit over time t. This can now be written as

$$\ddot{\lambda} = 3l\mathbf{e}_\rho \mathbf{e}_\rho{}^T \lambda - l\lambda \tag{36}$$

where $\lambda \equiv \begin{bmatrix} \lambda_u & \lambda_v \end{bmatrix}^T$. Multiply Eqn. (36) by $\mathbf{e}_\rho{}^T$ and $\mathbf{e}_\omega{}^T$, respectively to obtain

$$\mathbf{e}_\rho{}^T \ddot{\lambda} = 3l\mathbf{e}_\rho{}^T \lambda - l\mathbf{e}_\rho{}^T \lambda = 2l\mathbf{e}_\rho{}^T \lambda = 2\omega^2 \mathbf{e}_\rho{}^T \lambda \tag{37a}$$

$$\mathbf{e}_\omega{}^T \ddot{\lambda} = 3l\mathbf{e}_\omega{}^T \mathbf{e}_\rho \mathbf{e}_\rho{}^T \lambda - l\mathbf{e}_\omega{}^T \lambda = -l\mathbf{e}_\omega{}^T \lambda = -\omega^2 \mathbf{e}_\omega{}^T \lambda \tag{37b}$$

To complete the simplifications, it is necessary to obtain an expression for left-hand side of Eqn. (36) in terms of $\mathbf{e}_\rho$ and $\mathbf{e}_\omega$. That expression is

$$\ddot{\boldsymbol{\lambda}} = \frac{d^2}{dt^2}\left(\lambda_\rho \mathbf{e}_\rho + \lambda_\omega \mathbf{e}_\omega\right) = \frac{d}{dt}\left(\left(\dot{\lambda}_\rho - \omega\lambda_\omega\right)\mathbf{e}_\rho + \left(\dot{\lambda}_\omega + \omega\lambda_\rho\right)\mathbf{e}_\omega\right)$$
$$= \left(\ddot{\lambda}_\rho - 2\omega\dot{\lambda}_\omega - \omega^2\lambda_\rho\right)\mathbf{e}_\rho + \left(\ddot{\lambda}_\omega + 2\omega\dot{\lambda}_\rho - \omega^2\lambda_\omega\right)\mathbf{e}_\omega \tag{38}$$

Using this expression, Eqns. (37) become

$$\ddot{\lambda}_\rho - 2\omega\dot{\lambda}_\omega - \omega^2\lambda_\rho = 2\omega^2\lambda_\rho \tag{39a}$$

$$\ddot{\lambda}_\omega + 2\omega\dot{\lambda}_\rho - \omega^2\lambda_\omega = -\omega^2\lambda_\omega \tag{39b}$$

This can be represented with a matrix differential equation,

$$\begin{bmatrix} \dot{\lambda}_\rho \\ \dot{\lambda}_\omega \\ \dot{\lambda}_1 \\ \dot{\lambda}_2 \end{bmatrix} = \begin{bmatrix} 0 & 0 & 1 & 0 \\ 0 & 0 & 0 & 1 \\ 3\omega^2 & 0 & 0 & 2\omega \\ 0 & 0 & -2\omega & 0 \end{bmatrix} \begin{bmatrix} \lambda_\rho \\ \lambda_\omega \\ \lambda_1 \\ \lambda_2 \end{bmatrix} \tag{40}$$

where $\lambda_1 \equiv d\lambda_\rho/dt$ and $\lambda_2 \equiv d\lambda_\omega/dt$. The solution to this system is

$$\begin{bmatrix} \lambda_\rho \\ \lambda_\omega \\ \lambda_1 \\ \lambda_2 \end{bmatrix} = a\begin{bmatrix} 2 \\ -3\omega t \\ 0 \\ 3\omega \end{bmatrix} + b\begin{bmatrix} cos(\omega t) \\ -2\,sin(\omega t) \\ -\omega\,sin(\omega t) \\ -2\omega\,cos(\omega t) \end{bmatrix} + c\begin{bmatrix} sin(\omega t) \\ 2\,cos(\omega t) \\ \omega\,cos(\omega t) \\ -2\omega\,sin(\omega t) \end{bmatrix} + d\begin{bmatrix} 0 \\ 1 \\ 0 \\ 0 \end{bmatrix} \tag{41}$$

where a, b, c, and d are independent constants. The vector $\boldsymbol{\lambda}$ can be interpreted as the thrust direction in a reference frame fixed to the radius of the initial orbit, referred to here as the initial orbit reference frame. From the solution above, Eqn. (41), we see that there are four modes of the thrust direction. The mode associated with d is fixed with respect to the initial orbit reference frame. The mode associated with a is not fixed to that frame but is very simply described in it. The last two modes do not seem as well described in this frame.

To be sure, we would like to see that the approximate state dynamics given in Eqns (29) and (30) closely match those given in Eqns (3,4,5). To validate the approximate dynamics, it was simplest to simulate both systems using the same control. The most obvious choice for this control is the optimal control from the transfer in Fig.

7a. Figure 9 shows the results of the simulation. In this figure, "Delta-" states refer to the states from Fig. 7a with the initial orbit states subtracted, producing the desired plot for $\delta \mathbf{r}$. The "X1,Y1," etc. states refer to the states obtained by integrating Eqns. (30). The results seen in this figure are very promising: there is almost exact agreement between the two state histories. In fact, the worst error between the two at the end of the transfer is only about 1.5%.

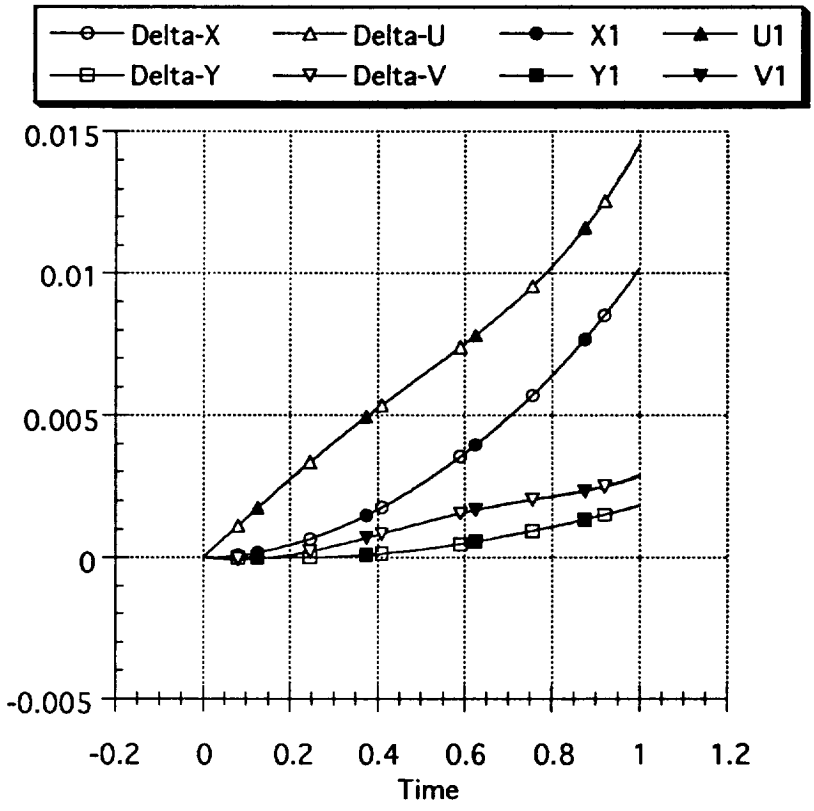

Figure 9: Validation Plot for the Dynamics in Equations (29) for the Transfer shown in Figure 7a

IV. CONCLUSIONS

The development of the Direction Correction Method is proceeding rather well. The ideas that it is based upon have been validated individually. At this point, the only weak link is the prediction of the new switching points. Testing of the method will be required in order to determine just how critical is the accuracy of that prediction.

The Patched Transfer Method is very promising. The dynamics resulting from assumptions made closely matches the dynamics before the approximations. Also, the simplicity of the resulting optimal control problem promises a state feedback guidance law. The usefulness of these results will outweigh the loss in accuracy. However, much more analysis must be performed to completely validate the linearized problem and its solution. Specifically, the approximate optimal control solution must be compared to exact solution; based on the agreement of the state, positive results are expected, but they must be verified.

V. REFERENCES

[1]Lawden, D.F., Optimal Trajectories for Space Navigation, Butterworths, London, 1963.

[2]Brusch, R.G. and Vincent, T.L., "Low-Thrust, Minimum-Fuel, Orbital Transfers," *Astronautica Acta*, Vol. 16, pp 65-74.

[3]Redding, D.C., "Optimal Low-Thrust Transfers to Geosynchronous Orbit," NASA Lewis SUDAAR 539, Cleveland, Ohio 44135, Sept. 1983.

[4]Oberle, H. J., BOUNDSCO - Hinweise zur Benutzung des Mehrzielverfahrens für die numerische Lösung von Randwerproblemen mit Schaltbedingungen, Hamburger Beiträge zur Angewandten Mathematik, Berichte 6, 1987.

[5]Chuang, C.-H., Goodson, T.G., and Hanson, J. "Theory and Computation of Optimal Low- And Medium-Thrust Orbit Transfers," AIAA Guidance, Navigation, and Control Conference Paper, September 1992.

[6]Zondervan, K.P., Lincoln, L.J., and Caughey, T.K., "Optimal Low-Thrust, Three-Burn Orbit Transfers with Large Plane Changes," *Journal of the Astronautical Sciences*, Vol. 32, No. 3, 1984, pp. 407-427

[7]Marec, J.P., Optimal Space Trajectories, Elsevier Scientific Publishing, New York, 1979.

[8]Glandorf, D.R., "Lagrange Multipliers and the State Transition Matrix for Coasting Arcs," *AIAA Journal*, Vol. 7, No. 2, Feb. 1969, pp 363-365.

[9]Eckenwiler, M. W., "Closed-Form Lagrangian Multipliers for Coast Periods of Optimum Trajectories," *AIAA Journal*, Vol. 3, No. 6, June 1965, pp 1149-1151.